Structured superhydrophilic coatings made from aminomalononitrile

Rou Jun Toh[1], Richard Evans [1], Helmut Thissen [1], Nicolas H. Voelcker [1,2,3], Marco D'ischia [4] and Vincent Ball [5,6,*]

[1] CSIRO Manufacturing, Research Way, Clayton 3168, Victoria, Australia
[2] Monash University, Monash Institute of Pharmaceutical Sciences, 381 Royal Parade, Parkville, 3052, Victoria, Australia
[3] Leibniz Institute for New Materials, Campus D2, 66123 Saarbrücken, Germany.
[4] Department of Chemical Sciences, University of Naples Federico II, Via Cinthia 26, 80126 Naples, Italy
[5] Université de Strasbourg, Faculté de Chirurgie Dentaire, 8 Rue Sainte Elizabeth, 67000 Strasbourg, France
[6] Institut National de la Santé et de la Recherche Médicale, Unité Mixte de Recherche 1121, 11 Rue Humann, 67085 Strasbourg, Cédex, France
* corresponding author: vball@unistra.fr

ABSTRACT

The motivation for new versatile and biocompatible coatings incites researchers to try to copy solutions developed by living organisms like mussels able to adhere to all kinds of substrates in wet conditions. Another source of inspiration may be found in molecules containing reactive CN groups which have been formed in prebiotic conditions on the early formed Earth. Among such molecules, aminomalonitrile (AMN) has been shown to allow the formation of coatings on all kinds of known materials. In the present investigation, the deposition mechanism of AMN based coatings on silicon, quartz and glass is investigated. It is shown that the film deposition is preceded by a lag phase during which AMN undergoes already a transformation in solution. The obtained coatings undergo a morphological transition from islands to fibrillar structures with a concomitant change in composition and hydrophilicity. A putative structure based on X-ray photoelectron spectroscopy data is proposed for the AMN based films deposited at the solid-water interface.

1. INTRODUCTION

Owing to the substrate specificity of most surface coating methodologies, surface scientists are investigating versatile surface chemistries. One major source of inspiration consists in biomimicry of mussel foot proteins (mefps) [1]. Indeed mussels are able to adhere to almost all known materials even in wet conditions and to withstand strong shear stresses which is a requirement for their survival. The composition of mefps, rich in L-lysine and in the non-natural amino acid L-DOPA, incited to use dopamine, containing an amino group as in L-Lysine and a catechol group as in L-DOPA, as a candidate to produce versatile and robust coatings in oxidative conditions [2, 3]. This led to the reproducible deposition of polydopamine films able to undergo easy secondary functionalisation

through reaction with nucleophiles [4] or with metal nanoparticles [2, 5] after reduction of metallic cations. Those polydopamine films are known to be useful for a lot of applications as coatings for biomaterials and for energy conversion processes [6]. Recently it was shown that inspiration from suspected prebiotic processes allows also to deposit conformal coatings on almost all known materials [7, 8] with application fields similar to those of polydopamine. The used precursor of such coatings is aminomalonitrile (AMN) which undergoes self-assembly and surface deposition after neutralisation of is para-toluenesulfonate salt in basic conditions. It is the aim of this article to summarize our mechanistic investigations [9] on the deposition of AMN based coatings and to show that those films also form at water-air interfaces and can be transferred on solid substrates via the

Langmuir–Schaeffer [10] horizontal transfer method. Most importantly, we will show that the AMN based colloids formed in solution, the films deposited at the water-solid interface and those deposited at the water-air interface are different. Additionally, the coatings deposited at the water-solid interface become superhydrophilic after a critical deposition time decreasing upon an increase in the AMN concentration.

2. MATERIALS AND METHODS

Chemicals

Aminomalononitrile-*para*-toluenesulfonate (AMN, ref. 221147), sodium hydrogen phosphate (ref. S-9638) and potassium hexacyanoferrate (ref. P9387) were purchased from Sigma-Aldrich and used without purification. All solutions were made from MilliQ water (ρ = 18.2 M$\Omega \cdot$cm, Millipore). AMN was dissolved in 50 mM sodium phosphate buffer at pH = 7.5 at concentrations ranging from 5 to 40 mg$\cdot$mL^{-1} corresponding to molar concentrations ranging from 19.7 mM to 158 mM. The reaction was triggered by adjusting the pH of these solutions to 8.6 $\pm$ 0.1 with a concentrated sodium hydroxide solution. Immediately after pH adjustment, cleaned samples to be coated were immersed in the AMN solution. The pH of all solutions was measured with a three point calibrated Hi221 pH meter (Hanna Instruments).

Substrate materials

AMN films were deposited on quartz, glass and silicon wafer samples, for characterization by means of UV-Vis spectroscopy, Langmuir-Blodgett transfer and ellipsometry, respectively. All of these substrates were cleaned in the same manner, just before deposition process. They were rinsed with ethanol, dried with a filtrated air flow and subjected to 15 min of O$_2$ plasma cleaning (PDC-32G-2, Harrick Scientific, USA).

UV-Vis spectroscopy

UV-Vis spectra of the AMN based films deposited on plasma cleaned quartz slides where obtained against a pristine cleaned quartz slide as a reference using a double beam mc² spectrophotometer (Safas, Monaco, France). The same spectrophotometer was used to measure the spectra of AMN solutions after different reaction times and appropriate dilution with sodium phosphate buffer, using the pure buffer as the reference. The solutions were contained in ethanol cleaned quartz cuvettes , 1 cm optical path (Thuet, Blodeslheim, France).

Ellipsometry

The AMN based films deposited for a reaction time *t* on freshly cleaned silicon substrates (featuring a naturally grown silicon dioxyde layer about 2 nm in thickness) were characterized by constant wavelength (632.8 nm) ellipsometry at a constant angle of incidence (70°) using a PZ 2000 ellipsometer (Horiba, France). For the calculation of the film thickness from the measured ellipsometric angles, the real part of the refractive index was fixed to 1.6 whereas its imaginary part was fixed equal to 0 owing to the film transparency at the used wavelength. The given thickness values are the average of 5 measurements (± one standard deviation) on regularly spaced spots along the major axis of the used wafer.

X-ray photoelectron spectroscopy (XPS)

The analysis of the AMN coated silicon slides was performed using an AXIS Ultra DLD spectrometer (Kratos Analytical, Manchester, UK) with a monochromated Al Kα source at a power of 168 W and a hemispherical analyser operating in the fixed analyser transmission mode and the standard aperture. The sample analysis area was 0.3 mm × 0.7 mm. Survey spectra were obtained at a pass energy of 160 eV. CasaXPS processing software version 2.3.15 (Casa Software Ltd., Teignmouth, UK) was used to perform data processing, with all elements present being identified from survey spectra. Calculation of the atomic concentrations of the detected elements were derived from integral peak intensities and the sensitivity factors supplied by the manufacturer.

Scanning electron microscopy (SEM)

SEM images were acquired by a Zeiss Gemini SEM 450 (Zeiss, Germany) at an acceleration voltage of 5 kV. Energy-dispersive X-ray spectroscopy (EDS) was carried out with an X-Max EDS system (Oxford Instruments, Oxford, UK) at an acceleration voltage of 15 kV. More details can be found in ref. [9].

Atomic force microscopy (AFM)

AMN based films deposited on silicon wafers from 10 mg·mL^{-1} AMN solutions were rinsed with distilled water and dried under a stream of filtered air before imaging in the contact mode with a MLCT-C cantilever (nominal spring constant = 10 mN·m^{-1}) using a Nanoscope III atomic force microscope (Bruker, Mannheim, Germany). Images were analysed with the Nanoscope Analysis software to determine the mean squared roughness of the AMN based films.

Contact angle measurements

For static water contact angle measurements, 5 µL distilled water was put on the surface of AMN based films deposited on plasma cleaned quartz slides. The contact angle was measured after 10 s using an Attension Theta goniometer (Biolin Scientific, Sweden). At least ten measurements were averaged to get a reliable value.

Langmuir-Schaeffer transfer of AMN based films from the liquid-air interface

AMN films were grown for 16 h or 23 h at the liquid-air interface from a 10 mg·mL^{-1} AMN solution. Part of the film was aspirated by a pipette and a cleaned glass slide mounted horizontally on a sample holder was immersed below the freshly created uncovered liquid-air interface, starting from the freed interface. The slide was then put below the apparent AMN film and the sample holder was removed in the upwards direction with a speed of 0.002 cm·s^{-1}. The films were then rinsed with pure water and dried under a flow of filtered air before AFM imaging in the dry state and in the contact mode as previously described.

2. RESULTS AND DISCUSSION

The initial pH of the AMN salt solution was lower than the initial pH of the 50 mM sodium phosphate buffer in an AMN concentration dependant manner.
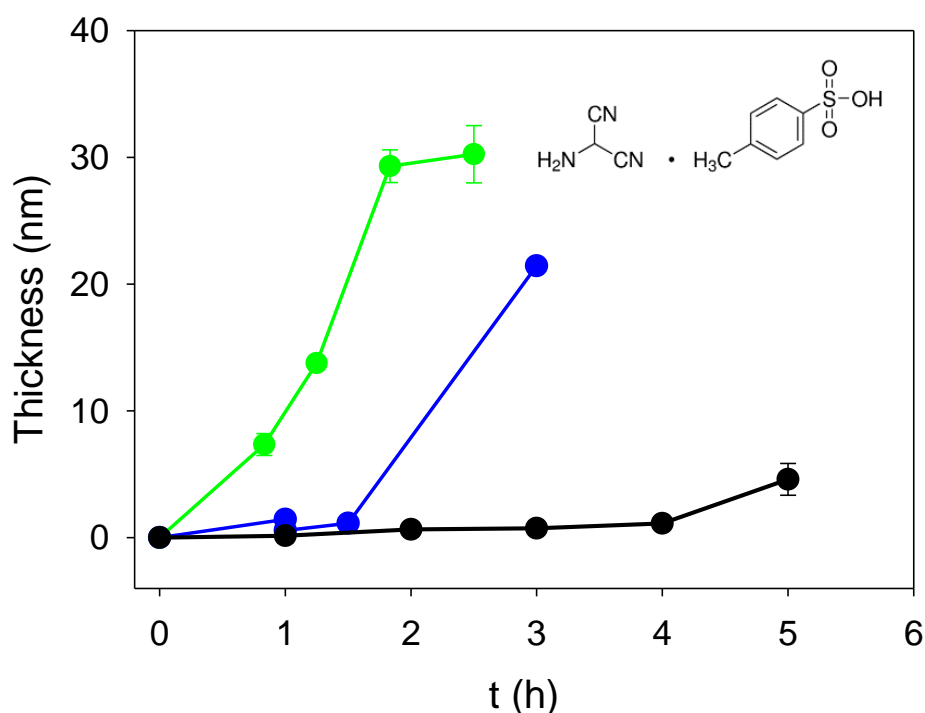

Figure 1. AMN based film thickness as measured by ellipsometry on silicon substrates from AMN solutions (initial pH = 8.6) at 5 (——), 10 (——) and 20 (——) mg.mL^{-1}. Each data point corresponds to an individual substrate and to the average ± one standard deviation over 5 different locations. The inset represents the structure of the used AMN salt. Modified from ref. [9] with authorization.

This decrease in pH stabilized AMN with respect to chemical transformation [9]. However titration of the AMN containing solutions to 8.6 with sodium hydroxide initiated a coloration change of the solution and a progressive deposition of a coating on both the reaction beaker and on the substrates immersed in it. The film deposition on solid substrates was delayed by an AMN concentration dependant lag phase as observed by means of single wavelength ellipsometry (Figure 1), UV-visible spectroscopy and quartz crystal microbalance with dissipation monitoring (data not shown, see ref.[9].
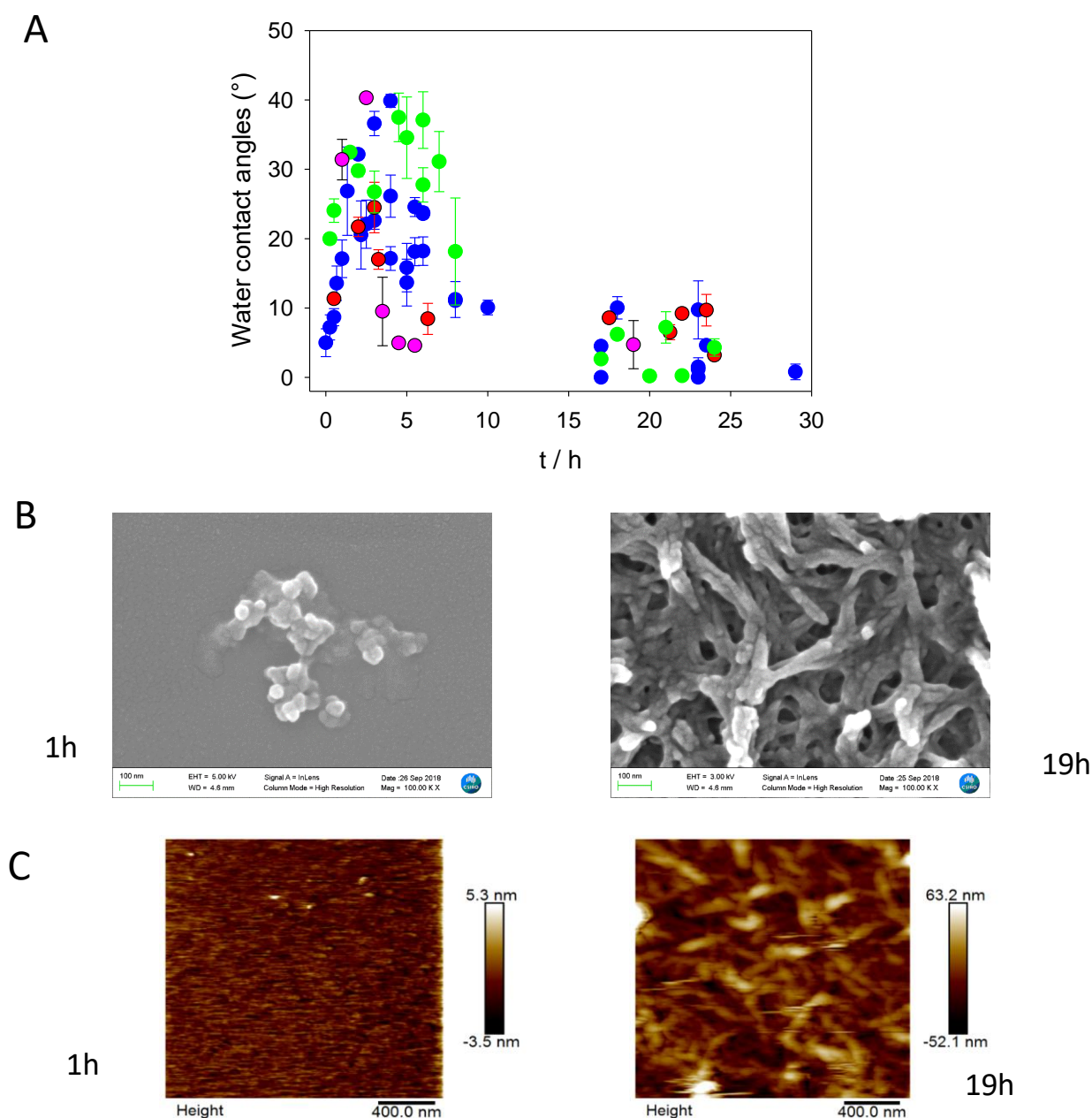

Figure 2. A : Static water contact angles of AMN based coatings as a function of time for different AMN concentrations : 5 (●), 10 (●), 20 (●) and 40 (●) mg·mL^{-1}.
B: Film morphology of AMN based coatings after 1 and 19 h of deposition from a 10 mg·mL^{-1} AMN solution as obtained by SEM.
C: Film morphology of AMN based coatings after 1 h and 19 h of deposition from a 10 mg·mL^{-1} AMN solution as obtained by contact mode AFM. The image size is 2 μm x 2 μm.

77

Nanomater. Sci. Eng., Vol. 2, No. 2, pp. 74-82 (2020)
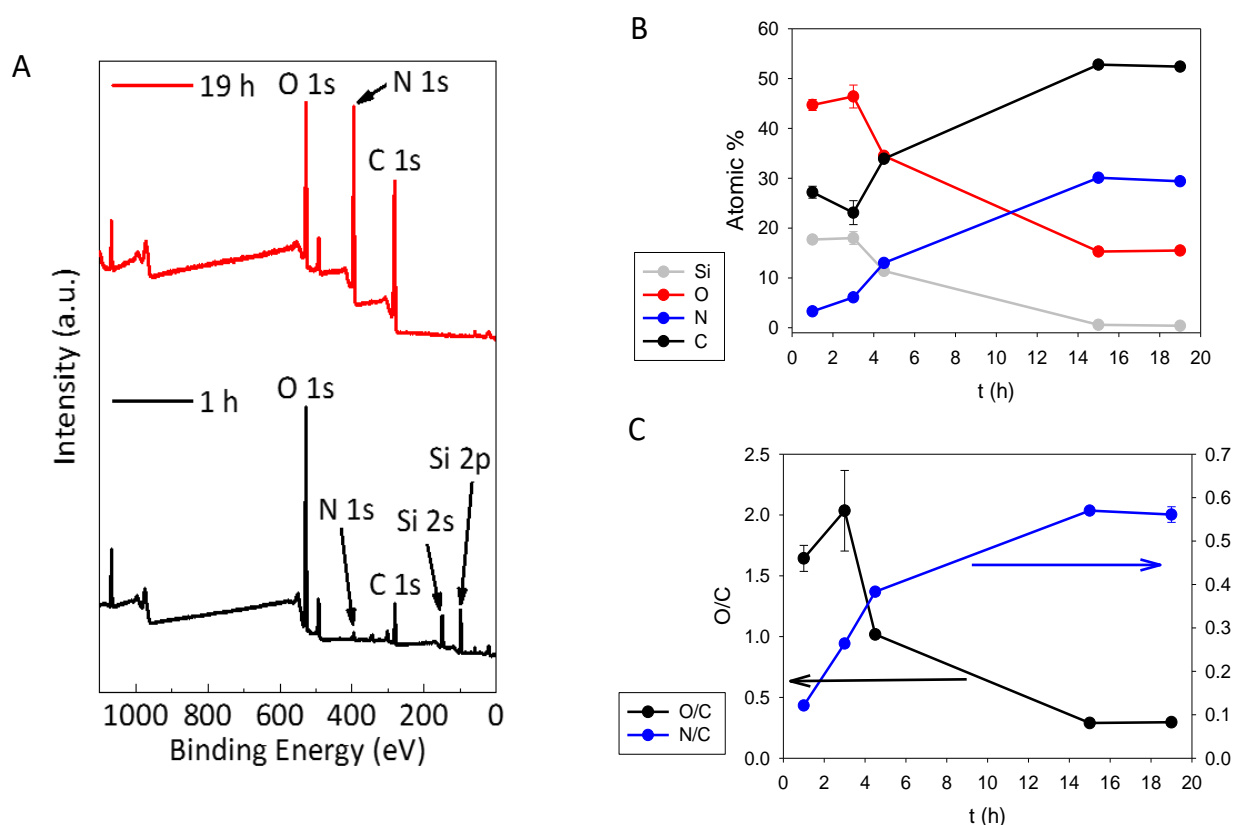
RESEARCH ARTICLE

Figure 3. A: XPS survey spectra of AMN based films after different deposition times (1 h and 19 h) on glass slides.
B: Evolution of the atomic percentage of Si (●), O (●), N (●) and C (●) as a function of time for AMN based coatings deposited in a 10 mg·mL^{-1} solution. The coatings were deposited on glass slides.
C: Evolution of the O/C (●) and N/C (●) ratios with reaction time in a 10 mg·mL^{-1} AMN solution. The error bars correspond to ± one standard deviation. Modified from ref. [9] with authorization.

The static water contact angles of the AMN based films passed through a maximum at intermediate deposition times and became progressively superhydrophilic (water contact angles lower than 10°) after intermediate deposition times. The higher the initial AMN concentration, the faster the superhydrophilic regime is reached (Figure 2 A). Such changes in surface wettability may be attributed to composition and/or surface roughness changes [11]. Concerning the surface topography of the AMN based coatings, SEM (Figure 2B) and AFM imaging (Figure 2C) clearly reveal an increase in surface roughness associated with the formation of fibrillary structures from initially deposited clusters (Figure 2B). Those fibrillar structures are formed after a few hours in the absence of any template

suggesting the self-assembly of anisotropic building blocks formed upon the reaction.

The morphology change is accompagnied by a modification in surface composition as shown by XPS spectroscopy (Figure 3). With increasing the deposition time, whatever the initial AMN concentration, the Si2S and Si2p photoelectrons due to the silicon substrates are not detected anymore highlighting the formation of conformal coatings. Those coatings were also found impermeable to a redox probe like potassium hexacyanoferrate [9]. Analysis of the obtained XPS spectra also reveals a progressive decrease of the O content of the films up to a constant value (Figure 3). Since O is present in the SiO_2 oxide film grown spontaneously on silicon, and since Si is not detected anymore when the O content reaches a steady state value, this means that the AMN based

78

General formula: $(C_3N_2O)_n$

N/C = 0.66
O/C = 0.33
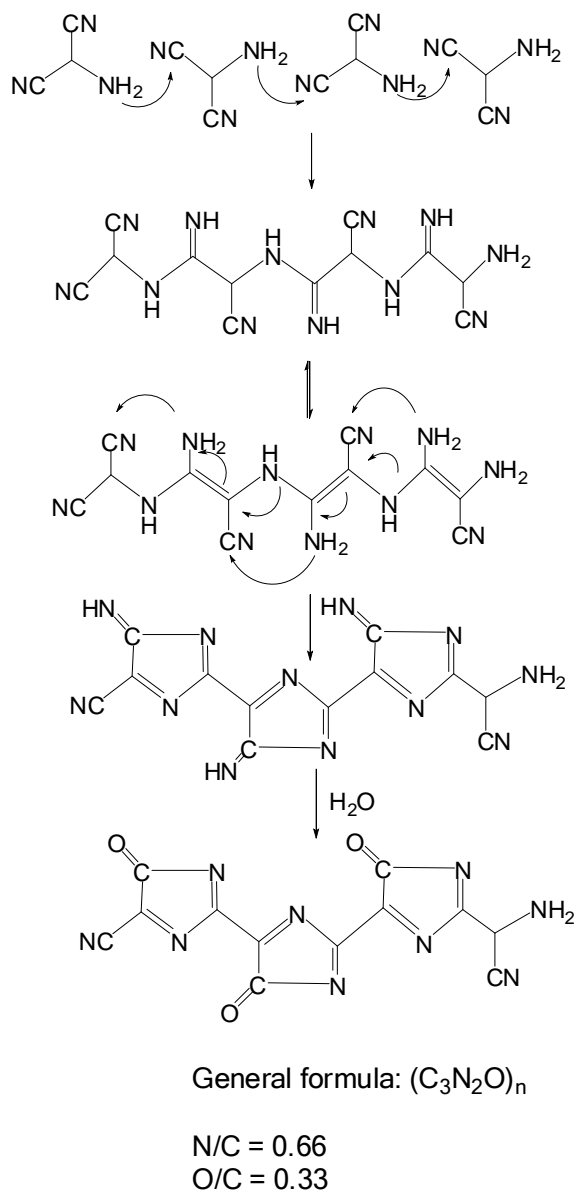
Scheme 1. Proposed structure of the polymeric material obtained at the solid-liquid interface from an AMN based solution at an initial pH of 8.6. Reproduced from ref.[9] with authorization.

films incorporate O which is not present in the AMN monomer (inset in Figure 1). This finding is important for inferring the film formation mechanism as described later on. The film deposition is also characterized by an increase in the surface concentration of C and N (Figure 3B). Interestingly the N/C atomic ration reaches a constant value of about 0.57 after prolonged deposition time (even if the film continues to grow up to this point) as in a previous investigation [7]. This C/N value is lower than the corresponding value for the AMN monomer which is equal to 1 (inset of Figure 1). This important finding means that some N is lost during the film deposition

independently from the CN- release detected in QCM-D experiments performed on gold: indeed a loss of film is detected with this gravimetric method when a gold substrate is put in contact with an AMN solution at an initial pH value of 8.6, meaning a release of CN- and subsequent partial dissolution of gold.

The simultaneous incorporation of O in the film and the C/N ratio close to 0.6 is interpreted by an hydrolysis reaction of the initially deposited film as shown in scheme 1 where the putative structure of the obtained material in given. Such a structure needs of course to be confirmed in future investigations.
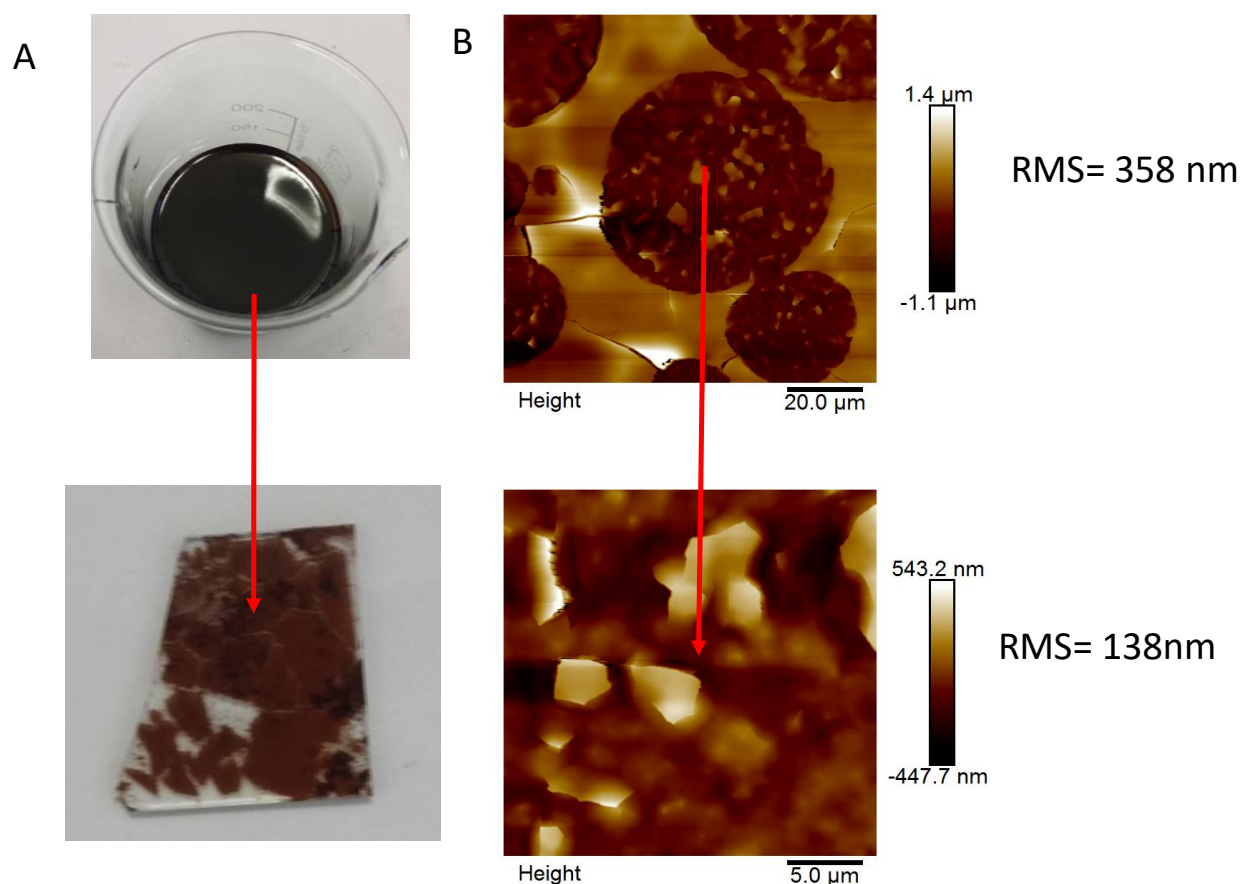
79

Nanomater. Sci. Eng., Vol. 2, No. 2, pp. 74-82 (2020)

RESEARCH ARTICLE

Figure 4. A: AMN based films on the liquid-air interface after 16 h of reaction (AMN at 10 mg·mL^{-1} at an initial pH of 8.6). Picture of the surface of the AMN containing solution after 16 h and after Langmuir Schaeffer transfer on a cleaned glass slide.
B: AFM surface topographies of the transferred AMN based film, the image size being 100 µm x 100 µm and 25 µm x 25 µm, respectively. The red arrow points to the region of the first image from which the image having a 25 µm x 25 µm size was acquired. Modified from ref. [9] with authorization.

Interestingly we also find that an AMN based film forms progressively on the water-air interface provided the AMN solution is not shaken (Figure 4A). This finding is in strong analogy with the situation of dopamine solutions in the presence of an oxidant [12] and strongly suggests that the the hydrophilic AMN transforms into amphiphilic structures which can self-assemble at the water-air interface. The final structure proposed in Scheme 1 is clearly amphiphilic with a hydrophobic chain decorated with hydrophilic CO groups. Those films deposited at the water-air interface can be transferred on cleaned glass slides through the Langmuir –Schaeffer method [10] and their morphology is drastically different (Figure 4b) than the morphology of AMN based films directly deposited on glass at the solid-water interface (Figure 2 B and C).

This finding suggests that the AMN film deposition mechanism is different at the solid-water and at the water –air interfaces, a point which clearly deserves further investigations. Complementarily, UV-visible spectra taken on quartz slides after a given duration of deposition and on diluted AMN containing solutions after the same reaction time are different (Figure 5A). This shows clearly that the film structure and / or composition is different than the composition of the AMN containing solution in which colloids form progressively with time, ending up with the sedimentation of precipitates. The evolution of AMN in solution proceeds also without a lag phase, contrarily to the film deposition (blue curve in Figure 5A, in agreement with the findings displayed in Figure 1).
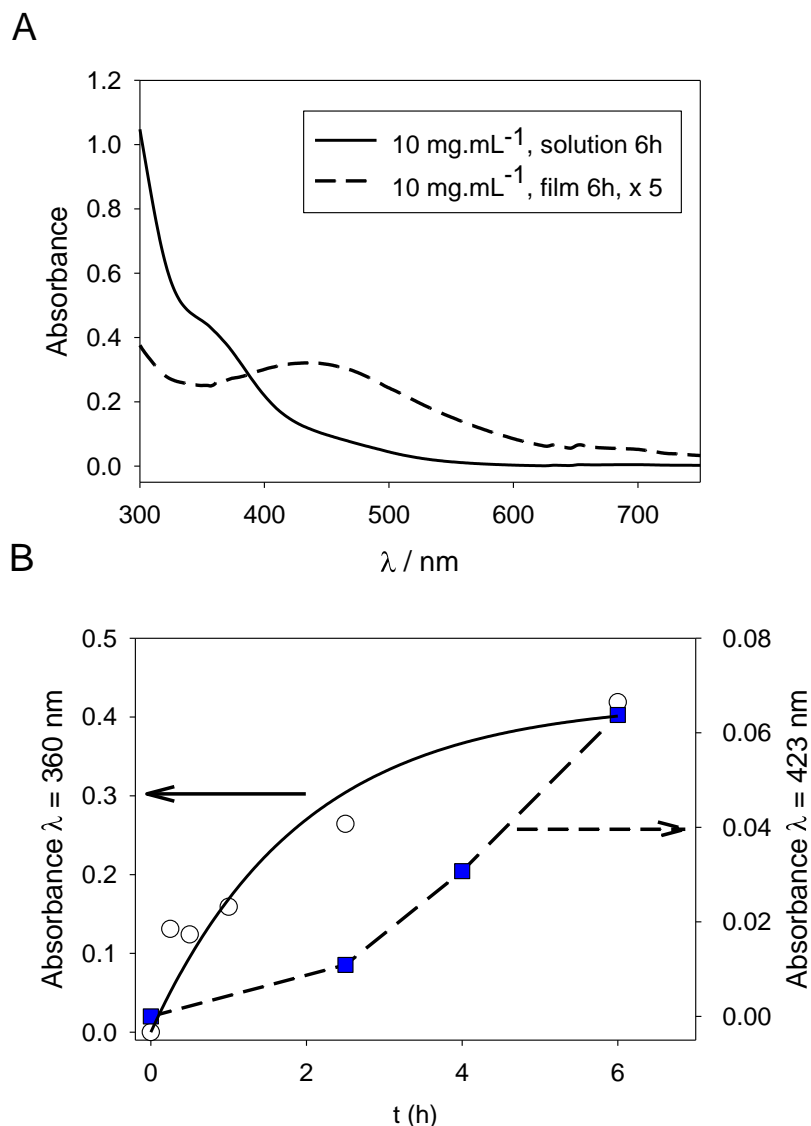
80

A

B

Figure 5. A: UV-Vis spectra of a 10 mg·mL^{-1} AMN solution (——) after 6 h of reaction and of an AMN film (– – –) deposited on a quartz wafer after the same reaction time, scaled by a factor of 5.
B: Time evolution of the absorbance at λ=360 nm (—O—, left hand vertical axis) and at λ=423 nm (– –■– – , right hand vertical axis) in the case of an AMN solution at 10 mg·mL^{-1} and for an AMN based film deposited from the same solution, respectively. Reproduced from ref.[9] with authorization.

4. CONCLUSIONS

The chemical evolution of the para-toluenesulfonate salt of AMN after its neutralization leads to the formation of conformal films on all kinds of substrates. Herein we focused on the film formation mechanism on quartz and glass substrates. It is found that the film deposition is preceeded by a lag phase whereas the chemical evolution of AMN in solution proceeds via a continuous pathway (Figure 5B). The obtained coatings at the solid-water interface undergo a morphological transition from islands to fibrillary structures accompagnied with the appearance of a superhydrophilic water wettability regime (Figure 3). In the same time the film composition changes (Figure 4). This lead us to propose a putative chemical structure compatible with the XPS compositional analysis (Scheme 1). Finally, we found that the chemical evolution/structural

81

Nanomater. Sci. Eng., Vol. 2, No. 2, pp. 74-82 (2020)

RESEARCH ARTICLE

evolution of AMN is different at the solid-water and water-air interfaces (Figure 4). Further investigations implying detailed NMR and X ray diffraction data (to relate the fibrillary film morphology to the self-assembly process) are required to understand the complex chemical pathways undergone by AMN in slightly alkaline solutions.

REFERENCES

[1] B.P. Lee, P.B. Messersmith, J.N. Israelachvili and J.H. Waite, *Ann. Rev. Mater. Res.*, **41**, 99-132 (2011).

[2] H. Lee, S.M. Dellatore, W.M. Miller and P.B. Messersmith, *Science*, **318**, 426-430 (2007).

[3] F. Bernsmann, V. Ball, F. Addiego, A. Ponche, M. Michel, J.J. de Almeida Gracio, V. Toniazzo and D. Ruch, *Langmuir*, **27**, 2819-2825 (2011).

[4] H. Lee, J. Rho and P.B. Messersmith, *Adv. Mater.*, **21**, 431 (2009).

[5] M. Lin, H. Huang, Y. Liu, C. Liang, S. Fei, X. Chen and C. Ni, *Nanotechnology* , **24**, art. 065501 (2013)

[6] Y. Liu, K. Ai and L. Lu, *Chem. Rev.* **114**: 5057-5115 (2014).

[7] H. Thissen, A. Koegler, M. Salwiczek, C.D. Eaton, Y. Qu, T. Lithgow and R.A. Evans, *NPG Asia Mater.*, **7**, art. e225 (2015).

[8] D.J. Menzies, A. Ang H. Thissen and R.A. Evans, *ACS Biomater. Sci. Eng.,* **3**, 793-806 (2017).

[9] R.J. Toh, R.A. Evans, H. Thissen, N.H. Voelcker, M. d'Ischia and V. Ball, *Langmuir*, **35**, 9896-9903 (2019).

[10] I. Langmuir and V.J. Schaefer, *J. Amer. Chem. Soc.* **58**, 284-287 (1936).

[11] D. Quéré, *Ann. Rev. Mater. Sci.* **38**, 71-99 (2008).

[12] F. Ponzio, P. Payamyar, A. Schneider, M. Winterhalter, J. Bour, F. Addiégo, M.-P. Krafft, J. Hemmerlé and V. Ball, *J. Phys. Chem. Lett.* **5**, 3436-3440 (2014).

82